ACS SENSORS

Article

pubs.acs.org/acssensors

Online Monitoring of Superoxide Anions Released from Skeletal Muscle Cells Using an Electrochemical Biosensor Based on Thick-Film Nanoporous Gold

Ramin Banan Sadeghian,[†,∥] Serge Ostrovidov,[†] Jiuhui Han,[†] Sahar Salehi,[†] Behzad Bahraminejad,[‡,∥] Hojae Bae,[§] Mingwei Chen,[†] and Ali Khademhosseini*[,†,§,∥,⊥,#,¶]

[†]WPI-Advanced Institute for Materials Research, Tohoku University, Sendai 980-8577, Japan

[‡]Department of Electrical Engineering, Faculty of Engineering, Majlesi Branch, Islamic Azad University, Esfahan 86316-56451, Iran

[§]College of Animal Bioscience and Technology, Department of Bioindustrial Technologies, Konkuk University, Hwayang-dong, Kwangjin-gu, Seoul 143-701, Republic of Korea

[∥]Biomaterials Innovation Research Center, Division of Biomedical Engineering, Department of Medicine, Brigham and Women's Hospital, Harvard Medical School, Boston, Massachusetts 02139, United States

[⊥]Harvard-Massachusetts Institute of Technology Division of Health Sciences and Technology, Massachusetts Institute of Technology, Cambridge, Massachusetts 02139, United States

[#]Wyss Institute for Biologically Inspired Engineering, Harvard University, Boston, Massachusetts 02115, United States

[¶]Department of Physics, Faculty of Science, King Abdulaziz University, Jeddah 21569, Saudi Arabia

Supporting Information

ABSTRACT: Online detection and accurate quantification of superoxide anions released from skeletal muscle tissue is important in both physiological and pathological contexts. Above certain physiologically redundant levels, superoxides may exert toxic effects. Here we present design, fabrication, and successful testing of a highly sensitive electrochemical superoxide biosensor based on nanoporous gold (NPG) immobilized with cytochrome-*c* (cyt-*c*). A significant 14-fold enhancement in the biosensor sensitivity was achieved using NPG instead of nonporous gold, enabling the device to quantify minuscule levels of superoxides. Such improvement was attributed to the very large surface-to-volume ratio of the NPG network. The average values of superoxide sensitivity and analytical limit of detection (LOD) were 1.90 ± 0.492 nA nM^{-1} cm^{-2} and 3.7 nM, respectively. The sensor was employed to measure the rates of superoxide release from C2C12 myoblasts and differentiated myotubes upon stimulation with an endogenous superoxide-producing drug. To account for the issue of sensor-to-sensor sensitivity variations, each sensor was individually calibrated prior to measurements of biologically released superoxides. For the drug concentrations studied, C2C12 superoxide generation rates varied from 0.03 to 0.2 pM min^{-1} $cell^{-1}$, within the range of superoxide release rates from normally contracting to fatiguing skeletal muscle tissue. Electrochemically obtained results were validated using a fluorescent superoxide probe. Compared to other destructive methods, the NPG-based electrochemical biosensor provides unique advantages in tissue engineering because of its higher sensitivity and the ability to measure the levels of biologically released superoxides in real-time.

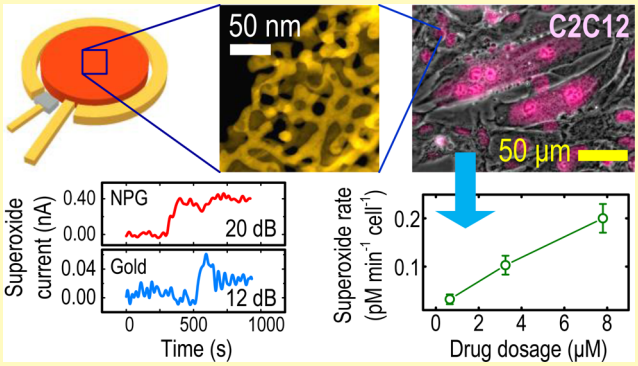

KEYWORDS: *electrochemical biosensor, nanoporous gold, reactive oxygen species, skeletal muscle cells, superoxide anions*

Since 1978 when the first evidence of physical exercise induced free radical mediated tissue damage was revealed, numerous studies have focused on the discovery of sources of free radical production and on developing efficient and accurate quantification techniques.[1−3] Free radicals such as reactive oxygen species (ROS), for instance, were mostly considered as toxic species involved in pathological states and mediators of muscle damage in dystrophy.[4] However, later on it was discovered that ROS at low levels are normal metabolites of cells functioning under physiological conditions.[5,6]

Among ROS, superoxides have gained considerable attention for their involvement in skeletal muscle tissue at rest and during contractile activity.[2,7,8] Superoxides normally experience disproportionation, yet they have a relatively longer half-life than other ROS, allowing them to move around the cell

Received: May 16, 2016
Accepted: June 14, 2016
Published: June 14, 2016

DOI: 10.1021/acssensors.6b00325
ACS Sens. 2016, 1, 921−928

targeting various organelles.[9] Nevertheless, they are rather impermeable through the plasma membrane (sarcolemma in particular),[2,10−12] making them difficult to detect in the extracellular milieu. Both the scarceness and the volatility of superoxides make it difficult to localize and measure them in small amounts that survive and are liberated.

Various techniques have been employed to evaluate skeletal muscle superoxides;[13−15] however, electrochemical methods are preferred because they are nondestructive, easy to implement, and sensitive in comparison, and they can provide real-time data without disturbing the cellular equilibrium.[16,17] Electrochemical biosensors incorporate superoxide-sensitive enzymes such as cytochrome-*c* (cyt-*c*) or a superoxide scavenger, superoxide dismutase (SOD) deposited directly onto the electrode or often anchored to the electrode via self-assembled monolayers (SAMs). Chen et al. carried out a comprehensive study on the performance of electrochemical superoxide sensors built on cyt-*c* immobilized onto a number of alkanethiol SAMs.[9] They showed that gold electrodes functionalized with cyt-*c* using dithiobis(succinimidyl)propionate (DTSP) as a linker offer the best balance between sensitivity and specificity. The Au/DTSP/cyt-*c* bioelectrode displayed a sensitivity of 0.41 nA nM^{-1} cm^{-2} and a low level of detection of 73 nM for superoxide in phosphate buffer. Later, Ganesana et al. functionalized a gold wire with cyt-*c* and measured the accumulation of superoxides in mouse brain slices in micromolar range with a sensitivity of 0.14 nA nM^{-1} cm^{-2} in culture medium.[11] Recently, Flamm et al. developed a cyt-*c*-based electrochemical microsensor capable of detecting the release of superoxides from T-47D human breast carcinoma cell line upon stimulation. The sensitivity of their device was 0.22 nA nM^{-1} cm^{-2}.[18]

Although these results are promising, the fatal effects of superoxide level changes in the cellular environment necessitate further improvement of the sensitivity of superoxide biosensors. Electrodes with immobilized cyt-*c*, although specific to superoxides and resistant to fouling, suffer from a reduced sensitivity.[9] A high sensitivity is particularly desirable when the signal to be identified is weak and a low limit of detection (LOD) is required. Measuring the dynamics of superoxide release from skeletal muscle tissues is an apt example. There has been a general lack of reports on accurate measurements of instantaneous superoxide production rates from monolayer cell cultures and skeletal muscle cells in particular, since such rates range from picomolar to nanomolar per minute.[12]

In the present study we utilized the large surface-to-volume ratio of NPG to achieve an enhanced sensitivity as reported earlier.[19,20] Moreover, the concept of using enzyme-immobilized NPG films in amperometric detection schemes has already been put forward.[21,22] Our NPG-covered electrodes once functionalized with cyt-*c* were able to detect and measure small levels of superoxides, with amplified and less noisy amperograms compared with nonporous gold electrodes having the same apparent surface area. After calibration, the set of biosensors were used to measure superoxide generation rates from stimulated C2C12 myoblast and myotube cultures as a function of stimuli concentration. A routinely used endogenous superoxide-producer, phorbol 12-myristate 13-acetate (PMA), was used as the stimulus.[23−27]

EXPERIMENTAL SECTION

NPG Synthesis and Characterization. NPG films were deposited on the working electrodes of screen-printed strips (DropSens, Spain) in a similar fashion to earlier works.[28,29] The working and counter electrodes of the strips were composed of low temperature sintered gold, while the reference electrode was of silver. Briefly, an $Ag_{82}Au_{18}$ layer was electrodeposited and then de-alloyed in a 1.0 M HNO_3 solution at room temperature for 20 min to remove the silver constituent, leaving behind the network of NPG (Figure S1). NPG-covered electrodes were thoroughly rinsed with deionized water (18 MΩ cm) to remove any traces of nitric acid and stored before being functionalized for superoxide detection. The electrochemically active surface areas (ESA) of the working electrodes before NPG deposition (hereafter referred to as unmodified) and after were assessed by conducting cyclic voltammetry in 0.5 M H_2SO_4 solution. In order to obtain the consumed charge, the area of the negative voltammogram lump corresponding to the reduction of AuO or Au(OH) to Au, was divided by the scan rate, 50 mV s^{-1}. The double-layer capacitance charge was then subtracted from the consumed charge resulting in a value proportional to the ESA. For more details refer to Figure S2 herein and to the work of Lu et al.[30]

Cell-Carrying Membranes. C2C12 myoblasts (passage number less than 5) were cultured in a medium comprising Dulbecco's Modified Eagle Medium (DMEM) (Gibco, USA), 1% penicillin−streptomycin (PS) (Sigma, USA), 10% fetal bovine serum (Biowest, Chile), and 20 mM 4-(2-hydroxyethyl)-1-piperazineethanesulfonic acid (HEPES) (Sigma, USA). At ∼70% confluency the cells were trypsinized and seeded at a density of 10^5 cells cm^{-2} onto 12-mm-diameter Corning Transwell porous polyester membranes containing 3-μm-wide pores (Sigma, USA). These membranes were detached from 12-well cell culture inserts. Immediately before seeding, the membranes were sterilized on each side for 15 min on a clean bench under UV light, placed in 30-mm-diameter tissue culture dishes, and soaked in sterile FNC Coating Mix (AthenaES, USA) for 30 s to enhance cell adhesion. After seeding, the membranes were incubated (30 min at 37 °C, 5% CO_2) so that the cells can settle and attach. Subsequently, 2 mL of culture medium was added to the cells and they were cultured for 2 days before performing the measurements. For the experiments with myotubes, after 2 days of culture the growth medium was switched to a differentiation DMEM medium containing 2% horse serum (Gibco, USA), 1% PS, and 20 mM HEPES and retained therein for 11 days. The differentiation medium was replaced every 2 days.

Electrode Functionalization. Both the unmodified and NPG-covered electrodes were functionalized as follows. An alkanethiol, dithiobis(sulfosuccinimidyl propionate) (DTSSP) (Dojindo, Japan) was used to covalently bond cyt-*c* (Sigma, USA) to gold. Briefly, the working electrode areas were drop-coated with 5 μL of DTSSP water-based solution (50 mM) and left in air flow for 20 min. We observed that such a high concentration of DTSSP guarantees formation of the SAM in a short time. It is known that the required immersion time decreases with concentration of the thiol solution.[31] Before the samples were completely dried, 5 μL of cyt-*c* solution (2 mM) in 1× phosphate-buffered saline (PBS) was dropped on the DTSSP-coated electrodes. The samples were sealed immediately, and incubated for 2 h at 37 °C to ensure immobilization and activation of the protein. The samples were then stored at 4 °C until usage no longer than 7 days.

Electrochemical Measurement Setup and Miscellaneous Quantification Experiments. The electrochemical measurement scheme is summarized in Figure S3. In addition, various immunostaining and fluorescent staining experiments were performed on cyt-*c*-immobilized electrodes and cell-carrying porous membranes for protein and cell visualization and quantification. Relevant procedures and results of such experiments are presented in Supporting Information. In addition, a superoxide specific fluorescent probe (MitoSOX, ThermoFisher Scientific, USA) was used to back up the electrochemically obtained results. Myotube-carrying porous membranes were immersed in a 5 μM HEPES-based solution of MitoSOX and incubated for 10 min at 37 °C. MitoSOX emits red fluorescence (excitation/emission ∼510/580) if oxidized by the superoxides. The intensity of fluorescence obtained from snapshots photographed from randomly selected areas of each sample were used as a measure of the concentration of superoxides.

DOI: 10.1021/acssensors.6b00325
ACS Sens. 2016, 1, 921−928

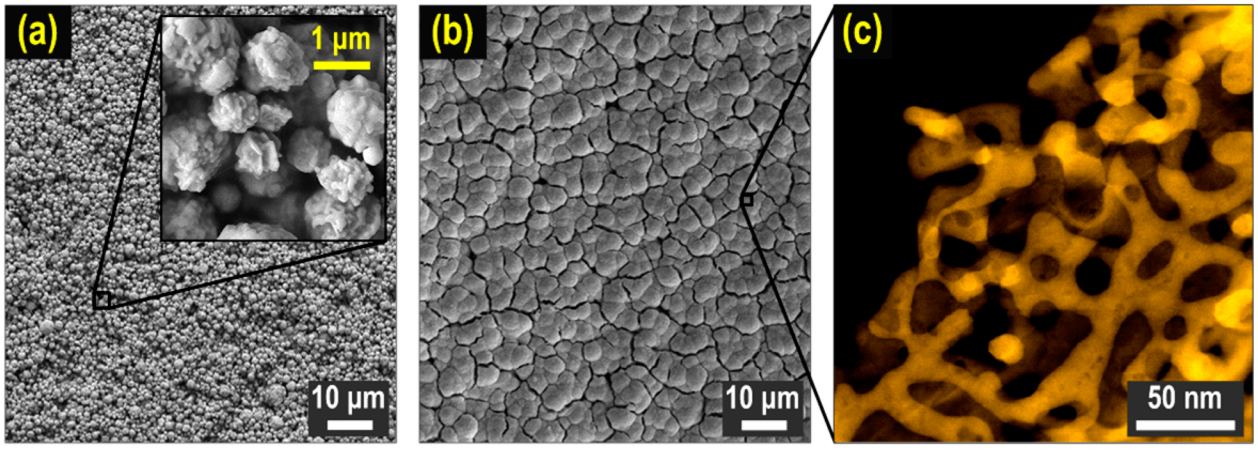

Figure 1. SEM micrographs showing the surface microstructure of (a) unmodified and (b) NPG-covered electrodes. (c) TEM image captured from delaminated NPG film showing the nanostructure of NPG with ligament/pore size of 20−30 nm (false color).

RESULTS AND DISCUSSION

Biosensor Fabrication, Characterization, And Calibration. The SEM images in Figure 1a and b show the surface structure of the unmodified and NPG-covered electrodes, respectively. The thickness of the electrodeposited NPG film was about 4 μm. Figure 2c shows a TEM micrograph of an NPG film flake peeled off the electrode surface. The nanoporous network of gold with average pore/ligament size of 20−30 nm is discernible. ESAs of the unmodified and NPG-covered electrodes were estimated by conducting cyclic voltammetry on three samples from each type. The voltammograms recorded from an unmodified and an NPG-covered electrode are shown in Figure 2a. Clearly the NPG-covered electrode has an effective surface area about 200 times wider (Figure 2b). Such an increase in the ESA is expected to result in an enhanced sensitivity for the NPG-based device.

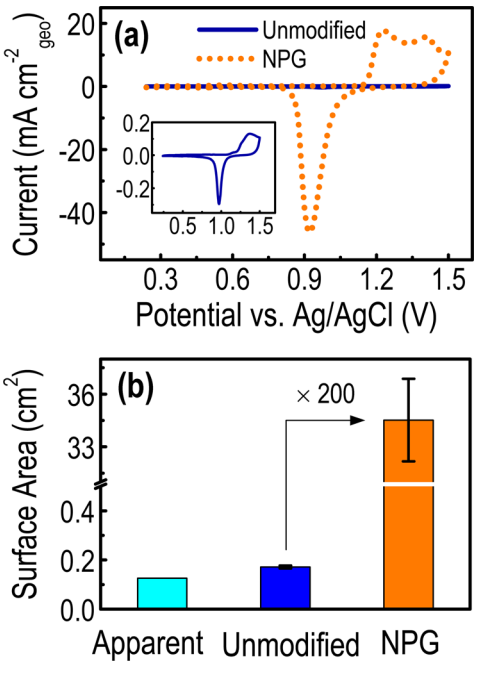

Figure 2. (a) Cyclic voltammograms of an unmodified (blue-solid curve) and a NPG-covered (gold-dotted curve) electrode. The charge consumed during the reduction of AuO or $Au(OH)_2$ is proportional to the electrode ESA and is obtained by integrating the reduction peak of the voltammograms. A magnified view of the unmodified electrode voltammogram is shown at the inset. (b) ESAs of unmodified and NPG-covered electrodes. The apparent surface area is 0.126 cm^2 for both.

Regardless of the electrode structure, both electrode types were functionalized with cyt-*c*, anchored to gold using a SAM of DTSSP. The DTSSP SAM attaches to gold via formation of the disulfide bond, while the activated *N*-hydroxysuccinimide (NHS) group at the other end of the molecule is readily attacked by the lysine residues of cyt-*c*. A variety of alkanethiols have been used to tether cyt-*c* to gold, among which DTSP[9] and DTSSP[26,27] appear to be the most suitable linkers. DTSSP has a higher efficiency for protein binding because of its stability against water, while DTSP is more prone to hydrolysis and is not as efficient at binding protein in an aqueous solution. Homogeneous coverage of cyt-*c* was examined visually and by immunostaining experiments (Figure S4).

Upon application of a positive bias the immobilized cyt-*c* (Fe^{3+}) is reduced to cyt-*c* (Fe^{2+}) by an impinging superoxide radical. The redox protein is subsequently reoxidized at the electrode surface producing current that is ideally proportional to the ambient superoxide concentration.

The biosensors were calibrated using the superoxides produced from the enzymatic reaction of xanthine and xanthine oxidase (XOD). It is well established that in saturated xanthine background superoxides are released with a concentration proportional to the square root of the enzyme activity, [XOD], as denoted by

$$[O_2^{\bullet -}] = \alpha [\mathrm{XOD}]^{1/2} \quad (1)$$

where $[O_2^{\bullet -}]$ is the concentration of superoxides in μM, [XOD] is in mU mL^{-1}, and the proportionality constant, α, is 3.95 μM mL$^{1/2}$ mU$^{-1/2}$ (For more details see Supporting Information, page S-5). Such dependence resembles dissociative absorption of H_2 into Pd lattice in the H−Pd system, where the resistance of palladium increases in proportion with the square root of the ambient hydrogen concentration also known as Sievert's law.[32]

Amperometric responses of representative biosensors with cyt-*c*-immobilized unmodified and NPG-covered electrodes to XOD aliquots are presented in Figure 3a. Although current peaks at the moment enzyme is added, a steady response is achieved once the superoxide-producing xanthine-XOD re-

DOI: 10.1021/acssensors.6b00325
ACS Sens. 2016, 1, 921−928

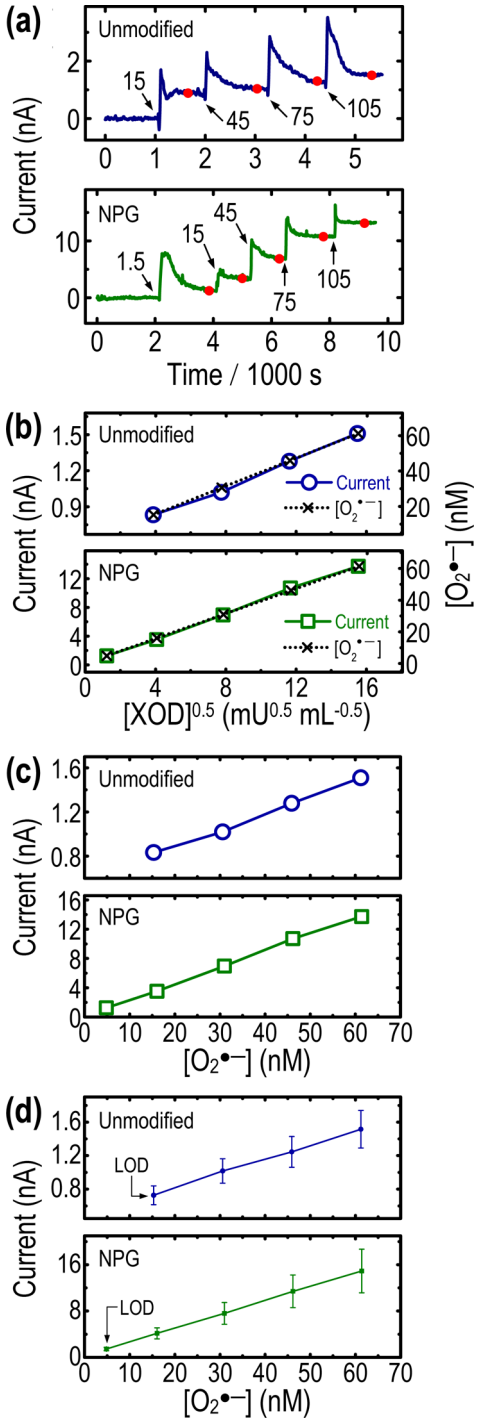

Figure 3. Biosensor calibration steps. (a) Representative amperometric responses to superoxide produced by sequential addition of XOD aliquots (in mU mL^{-1} as indicated by arrows) into xanthine solution after a baseline was achieved at 200 mV vs Ag reference electrode, for an unmodified electrode (top), and a NPG-covered electrode (bottom). Red dots designate the steady states. (b) Sievert-like output characteristics of the devices obtained from the corresponding amperograms in panel (a). (c) Transfer functions of the representative biosensors. (d) Average transfer functions (error bars represent the standard deviation of readouts for $n = 12$).

action reaches equilibrium. Currents did not decay during the course of chronoamperometry suggesting there is ample amount of dissolved oxygen and xanthine in the solution to sustain the reaction. The sensitivity of the biosensors were acquired from the magnitude of the redox current at steady-state (indicated by red dots in Figure 3a) and the corresponding [XOD] in the medium. [XOD] is 15 U mL^{-1} per each μL of the enzyme added to 500 μL of xanthine solution. As shown in the graphs of Figure 3b, current levels obtained from the curves of Figure 3a exhibited a linear dependence upon the square root of enzyme activity, $[XOD]^{1/2}$. Using eq 1, $[O_2^{\bullet-}]$ was computed and plotted against $[XOD]^{1/2}$ in the same graph. Biosensors transfer functions were extracted from these curves and depicted in Figure 3c. The transfer functions encompass superoxide concentration ranges of 15 to 61 nM and 5 to 61 nM of for biosensors with unmodified and NPG-covered electrodes, respectively. Biosensor sensitivity or gain, defined as the slope of transfer functions divided by the apparent surface area of the electrodes is expressed in nA nM^{-1} cm^{-2}. Through the aforementioned procedure, all the devices of both kind were calibrated individually and then interfaced with cells. The biosensors built on unmodified electrodes had an average sensitivity of 0.135 ± 0.024 nA nM^{-1} cm^{-2} while the sensitivity of the device with NPG-covered electrodes was 1.90 ± 0.492 nA nM^{-1} cm^{-2} as determined for 12 sensors of each type. Average amperometric transfer functions are presented in Figure 3d. LODs where estimated to be 19.7 nM and 3.7 nM for the unmodified and NPG based electrodes, respectively. As shown in Figure 3d, these values, correspond to superoxide concentrations generated by the lowest possible dose of XOD that could be reliably added to the saturated xanthine background (1.5 mU mL^{-1} for the NPG based device and 15 mU mL^{-1} for the unmodified electrode). Hence, the actual figures may even be smaller. We also calibrated NPG-covered electrodes without a cyt-*c* coating in the same manner, the results of which are presented and discussed in Supporting Information, page S-5.

The 14-fold increase in the gain, the smaller LOD, and an overall reduction in reproducibility can possibly be attributed to the higher electrode volume available for the diffusion of the analyte. However, the degree of such enhancement does not match the ESA values obtained by cyclic voltammetry experiments (Figure 2b). Initially, we suspected imperfect coverage of cyt-*c* and pore occlusion to play a part in such anomalous scaling of sensitivities, as the protein may not have diffused all the way into the NPG network leaving behind a portion of the gold unfunctionalized. As illustrated in Figures S5 and S6 such an assumption is confirmed by conducting cross-sectional SEM observations and energy dispersive X-ray spectroscopy (EDS) analysis. However, by comparing the superoxide sensitivities to those of bare NPG electrodes we concluded that it is the limited diffusion of the analyte through the pores that hinders obtaining a maximum sensitivity. Nevertheless, all the electrochemical measurements of biologically generated superoxides were carried using the biosensors with NPG-covered electrode.

In addition, we calibrated the devices toward H_2O_2 in order to examine possible interference of the analyte released after stimulating the cells. In a HEPES background, the hydrogen peroxide sensitivities acquired from eight devices of each kind were $(1.6 \times 10^{-4}) \pm (1.1 \times 10^{-4})$ and $(1.29 \times 10^{-3}) \pm (4.3 \times 10^{-4})$ nA nM^{-1} cm^{-2} for the unmodified and the NPG-covered electrodes, respectively. Peroxide gains happen to fall into the same range as reported earlier.[18] Based on these values the peroxide-to-superoxide cross sensitivities were 0.120% for the unmodified, and 0.068% for the NPG-covered set of electrodes.

DOI: 10.1021/acssensors.6b00325
ACS Sens. 2016, 1, 921−928

Measuring Superoxide Release Rates from Skeletal Muscle Cells. C2C12 myoblasts were seeded at a density of 10^5 cells cm^{-2} on porous polyester membranes and were used after 2 days of culture. These membranes were 10 μM thick and employed as a spacer between the cells and cyt-*c*, while allowing chemicals to pass through. A portion of the superoxides is inevitably recombined while traversing these membranes; however, this should not be an issue as we are interested in the rate of generation, not the absolute superoxide concentration.

For tests on myotubes, myogenesis was induced at day 2 of culture by switching the medium to a differentiation medium, after which the membranes were used at day 11 of differentiation.

HEPES was used for electrochemical measurements because of its superiority at maintaining physiological pH compared to other buffers such as PBS, and producing a smaller offset current. It was imperative to demonstrate that cell viability is not affected during the experiments mainly because dimethyl sulfoxide (DMSO) (Sigma, USA) was used as a solvent for PMA. Earlier studies using PMA as an oxidative burst activator suggests that the substance may not exert an unrecoverable toxic effect while the amount of DMSO should be of concern.[26] The concentration of the solvent was kept at or below 0.4% throughout our study, well below the lethal dose (about 1%).[33] We carried out live/dead tagging on myoblast-carrying porous membranes before and after a 1-h-long electrochemical experiment during which cells were triggered with 7.8 μM PMA dissolved in DMSO (0.4%). Results obtained from three samples indicate that viability was not affected at least after the test (Figure S7a,b).

The presence of myotubes was examined by immunostaining (Figure S7c). Usually, a fraction of myoblasts fail to convert to myotubes and remain as single nucleus proliferating cells. In order to eliminate nonfused proliferating myoblasts we administered an antiproliferative selective DNA synthesis inhibitor, Cytosine β-D-arabinofuranoside (Ara-C, Sigma, USA), at 4.1 μM,[34] at day 10 of differentiation, or 24 h prior to the measurements.

Cell cultures were stimulated with different concentrations of PMA while recording the biosensor response after a baseline was achieved. Five attempts were made for each PMA concentration. In a previous work we have shown that continuous superoxide generation is triggered by the drug exclusively, and not the DMSO solvent.[35] As shown in Figure 4a–c, superoxide generation rates were obtained from the slope of the amperograms once the current began to ramp up following administration of drug. These amperograms were recorded in HEPES background (500 μL) from myoblasts at day 2 of culture. Generation rates were computed by running linear regression over the signal during the initial 100 s of the ramp as indicated on the amperograms. The response of the same cells to 0.65 μM PMA captured by the unmodified electrode biosensor (Figure 4d) is clearly weaker and noisier than the signal acquired by the NPG-covered counterpart (Figure 4a). Wavelet de-noising method was applied in this study to extract the desired signal from the noise background.[36] Power signal-to-noise ratios (SNR) were 20.5 and 12.2 dB for the NPG-covered and the unmodified electrode biosensors, respectively. As mentioned earlier, the latter device fails to capture a sustained and reliable superoxide signal.

Also, due to the difficulty in reproducing protein-immobilized NPG-covered electrodes there was a relatively high variation of gain among the sensors (coefficient of variation = 25.9%). However, the problem was addressed by individual sensor calibration.

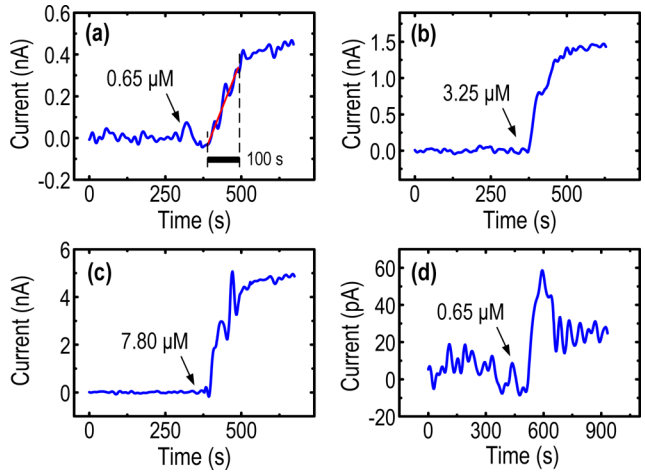

Figure 4. Instantaneous response of the NPG-covered electrode biosensor to superoxides generated from C2C12 cells, stimulated by PMA at (a) 0.65, (b) 3.25, and (c) 7.80 μM concentrations. (d) Response of the same cells to PMA captured by an unmodified electrode device.

The rates were assorted based on the concentration of PMA added to the medium. Figure 5a shows the values recorded from myoblasts at day 2 of culture, while Figure 5b,c displays the results obtained from myogenesis-induced cells at day 11 of differentiation, with and without Ara-C treatment, respectively.

Superoxide generation rates were normalized to the number of cell nuclei acquired from 10 cell-carrying membranes ($(4.14 \times 10^4) \pm 4500$ cells per membrane). Interestingly, the rates show a quasi-linear dependence upon drug concentration. In addition, there was no tangible difference in the measured rates between the myoblasts and the myogenesis-induced group, whether treated with Ara-C or not. Since cell counts were estimated separately, the error in such quantification was not incorporated in the normalized values.

Membranes carrying myotubes were treated by MitoSOX. PMA aliquots were added to the dyed cells and fluorescent snapshots were taken 1 min after the drug was administrated. Figure 5d shows the amounts of superoxides (not the release rate) obtained by analyzing the relative brightness of the fluorescent images, normalized to that of the basal case where no drug was added. Clearly, superoxide concentration increased with PMA dosage. Figure 5e compares the intensities of fluorescent snapshots taken from the dyed culture before and after PMA was added in two concentrations.

Although the degree of superoxide specificity of cyt-*c*-based sensors is scrutinized in the literature,[9,17] we carried out two separate tests to show that the amperometric response of the sensor is mostly due to reduction of the protein by the analyte. First, we used SOD (Sigma, USA) while the device was operating in the calibration mode (saturated xanthine–XOD system).

A bolus of SOD at 1000 U mL^{-1} was able to extinguish most of the superoxide signal (Figure S8a). Next, we incubated a myoblast-carrying membrane in a culture medium containing 200 U mL^{-1} of SOD for 1 h and then captured the sensor response while adding multiple doses of PMA. No superoxide signal was traced in the amperogram (Figure S8b).

DOI: 10.1021/acssensors.6b00325
ACS Sens. 2016, 1, 921–928

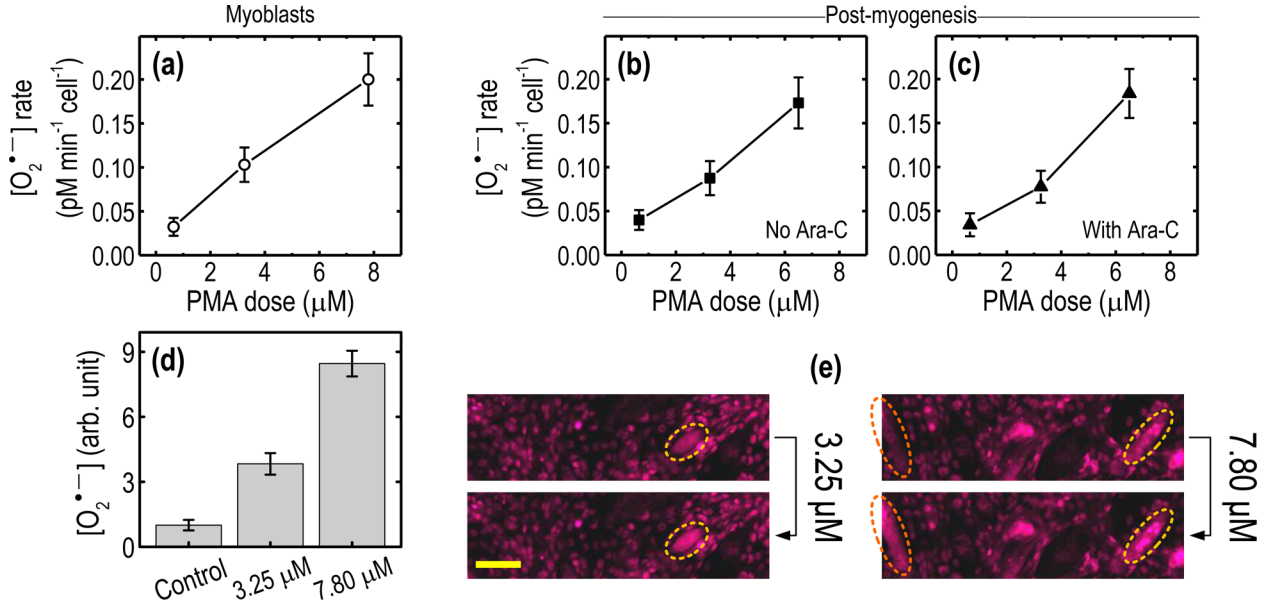

Figure 5. Superoxide generation rates as a function of PMA dosage. Electrochemically measured values using NPG-covered electrode biosensors from (a) myoblasts, (b) postmyogenesis cells as-cultured, and (c) postmyogenesis cells treated with Ara-C. Rates are normalized to the number of cell nuclei. (d) Normalized intensities of superoxides extracted from fluorescence snapshots taken 1 min after addition of PMA. (e) Increase in the fluorescence basal intensity upon application of PMA. Fluorescent images from MitoSOX-dyed (pink) myotubes differentiated on polyester membranes were snapped 1 min after PMA was added. Encircled areas reveal the relative increase in the brightness caused by the surge of superoxides. Five measurements were carried out to obtain each data point. The error bars indicate standard deviation. Scale bar is 100 μm.

To put the measurements into physiological perspective, earlier studies reporting on superoxide generation rates from similar tissues in vitro where revisited. Kobzik et al., for instance, showed that resting rat diaphragm bundles reduce cyt-*c* at a rate of 2.8 pM min^{-1} per mg of muscle.[37] This rate is known to increase about 7-fold to 19 pM min^{-1} mg^{-1} for an actively contracting muscle (6 contractions per min). Later on Kolbeck et al. revealed that fatiguing exercise can escalate the rate of superoxide production of the perfused rat diaphragm from a virtually negligible value, 10 pM min^{-1}, to 0.7 ± 0.17 nM min^{-1}, which is a 70-fold increase.[7] Düsterhöft et al. quantified mononucleated cells from skeletal muscles of the adult rat soleus and diaphragm, obtaining a yield of roughly 10^6 cells per gram of muscle.[38] Assuming that C2C12 cell densities are comparable (such an assumption is tenable as C2C12 cells are obtained from the thigh muscle of C3H mice), drug induced endogenous superoxide generation rates translate to 32 to 200 pM min^{-1} mg^{-1} (Figure 5a). This range is indeed within the same order recorded from normally contracting to fatiguing skeletal muscle tissue.

CONCLUSION

In comparison with a variety of other superoxide radical sensing methods, the electrochemical technique provides real-time data without disturbing the cellular metabolism; however, it is insensitive to minuscule amounts of superoxides released extracellularly. Thick films of ultraporous nanostructured gold prove to be a competent substitute for screen-printed electrodes in biosensing applications where a boost in sensitivity is required. Here we developed a sensitive superoxide radical electrochemical biosensor by functionalizing NPG films with a superoxide sensitive protein. To compensate for sensor-to-sensor gain variability, each device was calibrated individually before interfacing with cells. Instantaneous readouts of extracellular superoxide given off by skeletal muscle cells were obtained upon stimulation with an endogenous superoxide producer. We showed that superoxide generation rates ranging from 0.032 to 0.200 pM min^{-1} $cell^{-1}$ follow the concentration of the drug in a quasi-linear manner. These results confirm earlier reported measurements on a contractile skeletal muscle bundle. In addition, no tangible difference was observed in superoxide generation rates between undifferentiated and differentiated C2C12 cells. A fluorescence probe, MitoSOX, used to back up the electrochemically measured data, demonstrated a similar trend in the dependence of superoxide generation upon drug concentration.

ASSOCIATED CONTENT

Supporting Information

The Supporting Information is available free of charge on the ACS Publications website at DOI: 10.1021/acssensors.6b00325.

Schematic illustration of NPG electrode design; cyclic voltammetry approach to estimate electrode ESA; electrochemical measurement setup; evidence of cyt-*c* bounding to gold; biosensor calibration details, low limits of detection and, the dependence of electrode sensitivity upon surface coating; cross-sectional SEM and EDS observations; cell viability and myogenesis studies; superoxide-scavenging effect of SODs (PDF)

AUTHOR INFORMATION

Corresponding Author

* E-mail: alik@bwh.harvard.edu.

Notes

The authors declare no competing financial interest.

DOI: 10.1021/acssensors.6b00325
ACS Sens. 2016, 1, 921−928

■ ACKNOWLEDGMENTS

We would like to thank Prof. Susumu Ikeda for providing us with the Keithley 4200 semiconductor parameter analyzer.

■ REFERENCES

(1) Dillard, C. J.; Litov, R. E.; Savin, W. M.; Dumelin, E. E.; Tappel, A. L. Effects of exercise, vitamin E, and ozone on pulmonary function and lipid peroxidation. *J. Appl. Physiol Respir. Environ. Exerc. Physiol.* **1978**, *45*, 927−932.

(2) Powers, S. K.; Jackson, M. J. Exercise-Induced Oxidative Stress: Cellular Mechanisms and Impact on Muscle Force Production. *Physiol. Rev.* **2008**, *88*, 1243−1276.

(3) Fisher-Wellman, K.; Bloomer, R. J. Acute exercise and oxidative stress: a 30 year history. *Dyn. Med.* **2009**, *8*, 1−25.

(4) Matecki, S.; Fauconnier, J.; Lacampagne, A. Reactive Oxygen Species and Muscular Dystrophy. In *Systems Biology of Free Radicals and Antioxidants*, Laher, I., Ed.; Springer: Berlin Heidelberg, 2014; pp 3055−3079.

(5) Dröge, W. Free Radicals in the Physiological Control of Cell Function. *Physiol. Rev.* **2002**, *82*, 47−95.

(6) Tidball, J. G. Inflammatory processes in muscle injury and repair. *American Journal of Physiology - Regulatory, Integrative and Comparative Physiology* **2004**, *288*, R345−R353.

(7) Kolbeck, R.; She, Z.-W.; Callahan, L.; Nosek, A. Increased Superoxide Production during Fatigue in the Perfused Rat Diaphragm. *Am. J. Respir. Crit. Care Med.* **1997**, *156*, 140−145.

(8) Yavari, A.; Javadi, M.; Mirmiran, P.; Bahadoran, Z. Exercise-Induced Oxidative Stress and Dietary Antioxidants. *Asian J. Sports Med.* **2015**, *6*, e24898.

(9) Chen, X. J.; West, A. C.; Cropek, D. M.; Banta, S. Detection of the Superoxide Radical Anion Using Various Alkanethiol Monolayers and Immobilized Cytochrome c. *Anal. Chem.* **2008**, *80*, 9622−9629.

(10) Pearson, T.; Kabayo, T.; Ng, R.; Chamberlain, J.; McArdle, A.; Jackson, M. J. Skeletal Muscle Contractions Induce Acute Changes in Cytosolic Superoxide, but Slower Responses in Mitochondrial Superoxide and Cellular Hydrogen Peroxide. *PLoS One* **2014**, *9*, e96378.

(11) Ganesana, M.; Erlichman, J. S.; Andreescu, S. Real-time monitoring of superoxide accumulation and antioxidant activity in a brain slice model using an electrochemical cytochrome c biosensor. *Free Radical Biol. Med.* **2012**, *53*, 2240−2249.

(12) Murrant, C. L.; Reid, M. B. Detection of reactive oxygen and reactive nitrogen species in skeletal muscle. *Microsc. Res. Tech.* **2001**, *55*, 236−248.

(13) Palomero, J.; Pye, D.; Kabayo, T.; Spiller, D. G.; Jackson, M. J. In Situ Detection and Measurement of Intracellular Reactive Oxygen Species in Single Isolated Mature Skeletal Muscle Fibers by Real Time Fluorescence Microscopy. *Antioxid. Redox Signaling* **2008**, *10*, 1463−1474.

(14) Xu, X.; Thompson, L. V.; Navratil, M.; Arriaga, E. A. Analysis of Superoxide Production in Single Skeletal Muscle Fibers. *Anal. Chem.* **2010**, *82*, 4570−4576.

(15) Abdel Khalek, W.; Cortade, F.; Ollendorff, V.; Lapasset, L.; Tintignac, L.; Chabi, B.; Wrutniak-Cabello, C. SIRT3, a Mitochondrial NAD^+ -Dependent Deacetylase, Is Involved in the Regulation of Myoblast Differentiation. *PLoS One* **2014**, *9*, e114388.

(16) Manning, P.; McNeil, C. J. Electrochemical and optical sensing of reactive oxygen species: pathway to an integrated intracellular and extracellular measurement platform. *Biochem. Soc. Trans.* **2011**, *39*, 1288−1292.

(17) Calas-Blanchard, C.; Catanante, G.; Noguer, T. Electrochemical Sensor and Biosensor Strategies for ROS/RNS Detection in Biological Systems. *Electroanalysis* **2014**, *26*, 1277−1286.

(18) Flamm, H.; Kieninger, J.; Weltin, A.; Urban, G. A. Superoxide microsensor integrated into a Sensing Cell Culture Flask microsystem using direct oxidation for cell culture application. *Biosens. Bioelectron.* **2015**, *65*, 354−359.

(19) Seker, E.; Reed, M.; Begley, M. Nanoporous Gold: Fabrication, Characterization and, Applications. *Materials* **2009**, *2*, 2188−2215.

(20) Collinson, M. M. Nanoporous Gold Electrodes and Their Applications in Analytical Chemistry. *ISRN Anal. Chem.* **2013**, *2013*, 21.

(21) Stine, K. J.; Jefferson, K.; Shulga, O. V. Nanoporous Gold for Enzyme Immobilization. In *Enzyme Stabilization and Immobilization: Methods and Protocols*, Minteer, D. S, Ed.; Humana Press: Totowa, NJ, 2011; pp 67−83.

(22) Zhu, A.; Tian, Y.; Liu, H.; Luo, Y. Nanoporous gold film encapsulating cytochrome c for the fabrication of a H2O2 biosensor. *Biomaterials* **2009**, *30*, 3183−3188.

(23) Rist, R. J.; Naftalin, R. J. Glucose- and phorbol myristate acetate-stimulated oxygen consumption and superoxide production in rat peritoneal macrophages is inhibited by dexamethasone. *Biochem. J.* **1993**, *291*, 509−514.

(24) Tolias, C. M.; McNeil, C. J.; Kazlauskaite, J.; Hillhouse, E. W. Superoxide generation from constitutive nitric oxide synthase in astrocytes in vitro regulates extracellular nitric oxide availability. *Free Radical Biol. Med.* **1999**, *26*, 99−106.

(25) Hiatt, L. A.; McKenzie, J. R.; Deravi, L. F.; Harry, R. S.; Wright, D. W.; Cliffel, D. E. A printed superoxide dismutase coated electrode for the study of macrophage oxidative burst. *Biosens. Bioelectron.* **2012**, *33*, 128−133.

(26) Manning, P.; McNeil, C. J.; Cooper, J. M.; Hillhouse, E. W. Direct, Real-Time Sensing of Free Radical Production by Activated Human Glioblastoma Cells. *Free Radical Biol. Med.* **1998**, *24*, 1304−1309.

(27) Chang, S. C.; Pereira-Rodrigues, N.; Henderson, J. R.; Cole, A.; Bedioui, F.; McNeil, C. J. An electrochemical sensor array system for the direct, simultaneous in vitro monitoring of nitric oxide and superoxide production by cultured cells. *Biosens. Bioelectron.* **2005**, *21*, 917−22.

(28) Han, J.; Lin, Y.-C.; Chen, L.; Tsai, Y.-C.; Ito, Y.; Guo, X.; Hirata, A.; Fujita, T.; Esashi, M.; Gessner, T.; Chen, M. On-Chip Micro-Pseudocapacitors for Ultrahigh Energy and Power Delivery. *Advanced Science* **2015**, *7*, 1500067.

(29) Fujita, T.; Guan, P.; McKenna, K.; Lang, X.; Hirata, A.; Zhang, L.; Tokunaga, T.; Arai, S.; Yamamoto, Y.; Tanaka, N.; Ishikawa, Y.; Asao, N.; Yamamoto, Y.; Erlebacher, J.; Chen, M. Atomic origins of the high catalytic activity of nanoporous gold. *Nat. Mater.* **2012**, *11*, 775−780.

(30) Lu, Y.-C.; Gasteiger, H. A.; Shao-Horn, Y. Catalytic Activity Trends of Oxygen Reduction Reaction for Nonaqueous Li-Air Batteries. *J. Am. Chem. Soc.* **2011**, *133*, 19048.

(31) Love, J. C.; Estroff, L. A.; Kriebel, J. K.; Nuzzo, R. G.; Whitesides, G. M. Self-Assembled Monolayers of Thiolates on Metals as a Form of Nanotechnology. *Chem. Rev.* **2005**, *105*, 1103−1170.

(32) Hughes, R. C.; Schubert, W. K.; Buss, R. J. Solid-State Hydrogen Sensors Using Palladium-Nickel Alloys: Effect of Alloy Composition on Sensor Response. *J. Electrochem. Soc.* **1995**, *142*, 249−254.

(33) Wen, J.; Tong, Y.; Zu, Y. Low Concentration DMSO Stimulates Cell Growth and In vitro Transformation of Human Multiple Myeloma Cells. *Br. J. Med. Med. Res.* **2015**, *5*, 65−74.

(34) Vandenburgh, H.; Shansky, J.; Benesch-Lee, F.; Barbata, V.; Reid, J.; Thorrez, L.; Valentini, R.; Crawford, G. Drug-screening platform based on the contractility of tissue-engineered muscle. *Muscle Nerve* **2008**, *37*, 438−447.

(35) Banan-Sadeghian, R.; Ostrovidov, S.; Salehi, S.; Han, J.; Chen, M.; Khademhosseini, A. In *An Electrochemical Biosensor based on Gold Microspheres and Nanoporous Gold for Real-time Detection of Superoxide Anion in Skeletal Muscle Tissue*; IEEE EMBC, Milan, Italy, 2015; pp 7962−7965.

(36) Jansen, M. *Noise reduction by wavelet thresholding*; Springer Science & Business Media: New York, 2001; Vol *161*.

(37) Kobzik, L.; Reid, M. B.; Bredt, D. S.; Stamler, J. S. Nitric oxide in skeletal muscle. *Nature* **1994**, *372*, 546−548.

DOI: 10.1021/acssensors.6b00325
ACS Sens. 2016, 1, 921−928

(38) Dusterhoft, S.; Yablonka-Reuveni, Z.; Pette, D. Characterization of myosin isoforms in satellite cell cultures from adult rat diaphragm, soleus and tibialis anterior muscles. *Differentiation* **1990**, *45*, 185−191.

DOI: 10.1021/acssensors.6b00325
ACS Sens. 2016, 1, 921−928